Zdzisław GOSIEWSKI*

VIRTUAL RECOLLOCATION OF MEASUREMENT SIGNALS IN ACTIVE VIBRATION CONTROL SYSTEMS

SUMMARY

Collocation of sensors and actuators is an important feature of all motion control systems of active structures. Collocated systems provide great advantages from a stability, passivity, robustness and an implementation viewpoint. However it is not always possible to collocate the control actuators with sensors. Active magnetic bearings (AMBs) are examples of such systems. The paper presents a new method for recollocating the axes or planes of measurement to the axes or planes of actuation. Applying methods known from the control systems theory, such as state-space models, observers and transformations to canonical forms it is possible to calculate the transformation matrix that recollocates the measurement signals from the locations of sensors to the locations of actuators. The approach is illustrated with an analytical and numerical example of a rigid rotor supported by AMBs. The results confirm the correctness of the proposed method.

***Keywords**: measurement signals, control signals, mechanical structures, collocations*

*WIRTUALNA REKOLOKACJA SYGNAŁÓW POMIAROWYCH
W UKŁADACH AKTYWNEGO STEROWANIA DRGANIAMI*

Kolokacja (współosiowość, współpłaszczyznowość) elementów pomiarowych i wykonawczych jest ważną zaletą w układach sterowania drganiami podatnych konstrukcji mechanicznych. Niekolokacja tych elementów powoduje, że konstrukcja może, z punktu widzenia teorii sterowania, stać się obiektem nieminimalnofazowym, a więc trudnym do wysterowania.

W artykule zaproponowano metodę uzyskiwania kolokacji przez odpowiednie przekształcanie wartości sygnałów pomiarowych. Zarówno dla rzeczywistych pomiarów, jak i dla wirtualnych pomiarów zgodnych z kierunkami działania elementów wykonawczych model obiektu przekształcany jest do postaci kanonicznej obserwowalnej. Oba modele równania pomiarów są ze sobą porównywane i wyznaczana jest transformacja sygnałów. Aby uzyskać pełną informację o przekształcanym wektorze stanu, dokonuje się jego estymacji przez zastosowanie obserwatora zredukowanego rzędu.

Rozważania teoretyczne poparte zostały przykładem analitycznym i numerycznym, w którym jako obiekt sterowania wykorzystano wirnik sztywny łożyskowany magnetycznie.

***Słowa kluczowe**: elementy pomiarowe, elementy wykonawcze, kolokacja, wirnik, łożyska magnetyczne*

1. INTRODUCTION

Vibration control systems of mechanical structures can be collocated or non-collocated. When a sensor is placed at the same location as the input force, i.e. when all input forces have instant and distinguishable influence on the measurement signals, the system is said to be collocated. The collocated problems have unique solutions and are said to be *well-posed* (Nordstrom and Nordberg 2004). However, in many real life mechanical systems it is not possible to collocate the vibration control actuator at the location of interest. As an example, consider active magnetic bearing (AMB). Eddy current sensors are frequently used in this case to measure the shaft displacements. However, the shaft segment of the given diameter and some distance between sensors and the rest of the magnetic circuit is required for the proper operation of the AMB. This is why it is not possible to collocate the sensors and actuators. Sometime we need the information about structure motion in another points than the measured points. The robot with flexible arms is a good example. In earlier papers to avoid problems connected with sensor location the modal filters (Meirovitch and Baruh 1983) or averaging filters (Weng *et al.* 2002) were considered.

Non-collocation complicates the control problem because the dynamics of the structure between the control actuator and sensor disturbs the performance of the vibration control system. It has been proved, that the non-collocated systems have non-minimum-phase zeros (Preumont 2002). These zeros can increase the sensitivity of the control system to parameter variation. Furthermore, if these zeros occur within the operating range of the system, the system can become unstable (Qui *et al.* 2009).

The non-collocation effects on the stability of the vibration control system can be suppressed by several ways. Qiu *et al*. (Qui *et al.* 2009) employed the phase shifting approach for the cantilevered flexible beam model with non-collocated piezoelectric actuator and accelerometer. This approach was effective in suppressing the first two bending modes of the beam. Nordstrom and Nordberg

* Bialystok University of Technology, Faculty of Mechanical Engineering

(2004), proposed a time delay method to solve non-collocated input estimation problems. They showed that introducing a time delay can improve the input estimation considerably. Buhr *at al.* (1997), considered a non-collocated passive vibration absorber for vibration attenuation. However, the absorber was found to be uncontrollable for certain frequencies, so a feedback based tuning algorithm for a variable stiffness vibration absorber was developed.

The present paper recommends the *virtual* (recalculated) collocation. Its origin is in paper (Gosiewski 2010) in which it was found that in the case of a four-mode rigid rotor it is possible to collocate input-output signals using a simple transformation of measured signals. Next, this approach was extended on flexible rotors with a reduced number of modes considered (Gosiewski *et al.* 2010). Unfortunately, such simple approach is possible only in the case when the number of sensors equals the number of considered modes. Therefore in the present paper, the control theory is applied to obtain the collocation. The idea is to calculate the displacements at the actuator locations having the measured displacements at the sensors locations or, to calculate the control forces at the actuator locations having the displacements measured at the sensor locations. This paper discusses the former method, as it is a common practice to design the local control loops rather than the global ones (Preumont 2002). The analytical formulas for such approach are developed, based on the control system theory. By transforming the controlled system to its observable and controllable canonical forms, the simple dependencies for sensors and actuators virtual recollocation can be obtained. The reduced-order observer was designed to estimate the state vector in its controllable canonical form. The full algorithm of the recollocation method is finally presented. The proposed method is illustrated by the analytical example where the rigid rotor is a considered plant. Results of numerical simulation confirm possible potential of the proposed recollocation method and give a rationale for its further investigations.

2. NONCOLLOCATED SYSTEM AND ITS MODEL

Let us consider the mechanical dynamic system described as follows

$$\mathbf{M}\ddot{\mathbf{q}} + \mathbf{C}\dot{\mathbf{q}} + \mathbf{K}\mathbf{q} = \mathbf{f} + \mathbf{B_c u} \tag{1}$$

where **q** and **f** are vectors of generalized (translational and rotational) co-ordinates and generalized external forces (forces and force moments), respectively, **u** are controlling signals. **M**, **K**, and **C** are matrices of mass, flexibility and damping, respectively, $\mathbf{B_c}$ is control matrix in Cartesian frame of coordinates.

Introducing modal matrix: $\mathbf{\Phi} = (\phi_1, \phi_2, .., \phi_n)$, and taking into account ortogonality conditions: $\mu = \mathbf{\Phi}^T \mathbf{M\Phi} = \mathrm{diag}(\mu_i)$, $\mathbf{\Phi}^T \mathbf{K\Phi} = \mathrm{diag}(\mu_i \omega_i^2)$, and Raleigh hypothesis $\mathbf{\Phi}^T \mathbf{C\Phi} = \mathrm{diag}(2\xi_i \mu_i \omega_i)$ we rearrange the equation (1) to the diagonal form:

$$\ddot{z} + 2\xi\Omega\dot{z} + \Omega^2 z = \mu^{-1}\Phi^T f + \mu^{-1}\Phi^T B_c u \tag{2}$$

where:

$\mathbf{z} = \mathbf{\Phi x}$ – modal coordinates,
μ_i – i-th modal mass,
ω_i – i-th natural frequency,
ξ_i – i-th modal damping coefficient.

When the system is harmonically excited and external forces are nullified: $\mathbf{f} = \mathbf{0}$, it answers with the same frequency: $\mathbf{q} = \mathbf{Q}e^{j\omega t}$. We assume, the vibrations are measured in points described by formula:

$$\mathbf{y} = \mathbf{Mq} \tag{3}$$

So, the complex input-output amplitudes are connected according to equation (1) by the following formulae:

$$\begin{aligned}\mathbf{Y} = \mathbf{MQ} &= \mathbf{M}\left[-\omega^2\mathbf{M} + j\omega\mathbf{C} + \mathbf{K}\right]^{-1}\mathbf{BU} = \\ &= \mathbf{MG}_K(\omega)\mathbf{BU} = \mathbf{G}_m(\omega)\mathbf{U}\end{aligned} \tag{4}$$

The matrix $\mathbf{G}_K(\omega)$ is a dynamic form of the compliance matrix $\mathbf{K}^{-1}$, while $\mathbf{G}_M(\omega)$ is a transfer function. The modal model has also coordinates with complex amplitudes: $\mathbf{z} = \mathbf{Z}e^{j\omega t}$. In such case the equation (2) has solution in the form:

$$\mathbf{Z} = \mathrm{diag}\left\{\frac{1}{\mu_i(\omega_i^2 - \omega^2 + 2j\xi_i\omega_i\omega)}\right\}\mathbf{\Phi}^T\mathbf{B_c U} \tag{5}$$

so in cartesian coordinates we have:

$$\begin{aligned}\mathbf{Y} = \mathbf{MQ} &= \mathbf{M\Phi Z} = \\ &= \mathbf{M\Phi}\mathrm{diag}\left\{\frac{1}{\mu_i(\omega_i^2 - \omega^2 + 2j\xi_i\omega_i\omega)}\right\}\mathbf{\Phi}^T\mathbf{B_c U}\end{aligned} \tag{6}$$

Comparing equations (4) and (6) , we obtain the transfer function which can be expressed in the form of modal sum:

$$\begin{aligned}\mathbf{G_K}(\omega) &= [-\omega^2\mathbf{M} + j\omega\mathbf{C} + \mathbf{K}]^{-1} = \\ &= \sum_{i=1}^{n} \frac{\phi_i\phi_i^T}{\mu_i(\omega_i^2 - \omega^2 + 2j\xi_i\omega_i\omega)}\end{aligned} \tag{7}$$

where a single component represent the dynamics of the single vibration mode. Assume the system has $l = 1, 2, ..., p$ inputs (controlling signals) and $k = 1, 2, \ldots, r$ outputs (sensors). In such a case the transfer function has the form:

$$\mathbf{G}_m(\omega) = \mathbf{MG}_K(\omega)\mathbf{B} = \sum_{i=1}^{n} \frac{\phi_i(k)\phi_i^T(l)}{\mu_i(\omega_i^2 - \omega^2 + 2j\xi_i\omega_i\omega)} \tag{8}$$

where the location of matrix element is indicated by the k and l. When the sensors and controlling signals are located in opposite sides of the mode node some residua in transfer function are negative. It can lead to the non-minimumphase model of the vibration system since there can arrive the transfer function zeros with positive real part. Such system is called non-collocated and it is difficult to control. It will be illustrated in the next chapter.

3. ROTOR-MAGNETIC BEARINGS SYSTEM

In magnetically suspended rigid rotor the control system has usually 5 control axes – four radial and one axial, respectively. The radial control axes are coupled and rotor motion can be described by modal coordinates (Preumont 2002), which present translation vibrations of the rotor mass centre – x, y, and rotation vibrations (tilting of the shaft) – α, β. Modal coordinates are completed into vector: $\mathbf{p}=\begin{bmatrix} x & \beta & y & -\alpha \end{bmatrix}^T$.

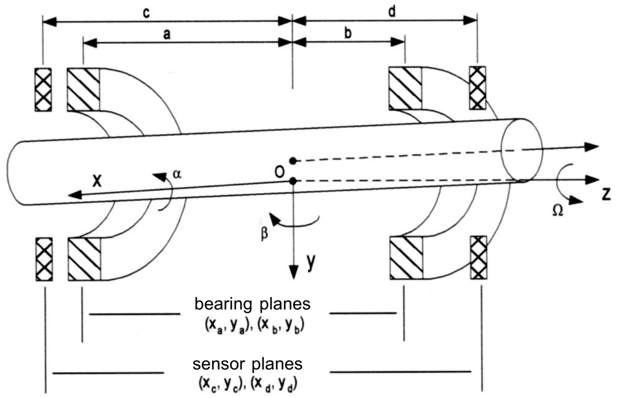

Fig. 1. Scheme of the rotating system with two radial magnetic bearing planes and sensor planes

To simplify calculations it is assumed that sensor and bearing planes cover each other (Fig. 1). In this case all motion equations can be written in the matrix form:

$$\begin{bmatrix} \mathbf{M} & \mathbf{0} \\ \mathbf{0} & \mathbf{M} \end{bmatrix}\ddot{\mathbf{p}} + \Omega I_z \begin{bmatrix} \mathbf{0} & \mathbf{G} \\ -\mathbf{G} & \mathbf{0} \end{bmatrix}\dot{\mathbf{p}} = \begin{bmatrix} \mathbf{T}_b^T & \mathbf{0} \\ \mathbf{0} & \mathbf{T}_b^T \end{bmatrix}\mathbf{F} \tag{9}$$

where:

$$\mathbf{M} = \begin{bmatrix} m & 0 \\ 0 & I_x \end{bmatrix},\ \mathbf{G} = \begin{bmatrix} 0 & 0 \\ 0 & 1 \end{bmatrix},\ \mathbf{T}_b = \begin{bmatrix} 1 & -a \\ 1 & b \end{bmatrix},$$

$$\mathbf{F} = \begin{bmatrix} F_{ax} & F_{bx} & F_{ay} & F_{by} \end{bmatrix}^T.$$

In above formulae:

- F – electromagnetic forces where indices $(_{a,\ b})$, $(_{x,\ y})$ indicate proper bearing plane and proper axis in the plane,
- m – mass,
- a, b – distances of the rotor mass centre from the bearing planes, respectively, where: $a+b = l$,
- Ω – rotor angular speed,
- $I_x = I_y, I_z$ – moments of inertia with respect to axes: x, y, z.

The rotor motion should be expressed by rotor co-ordinates in the bearing planes $\mathbf{p}_b = \begin{bmatrix} x_a & x_b & y_a & y_b \end{bmatrix}^T$ or in measurement planes $\mathbf{p}_m = \begin{bmatrix} x_c & x_d & y_c & y_d \end{bmatrix}^T$ by transformation (Gosiewski and Falkowski 2003):

$$\begin{aligned} \mathbf{p}_b &= \mathbf{T}_1\mathbf{p}, \\ \mathbf{p}_m &= \mathbf{T}_2\mathbf{p}, \end{aligned} \tag{10}$$

where:

$$\mathbf{T}_1 = \begin{bmatrix} \mathbf{T}_b & \mathbf{0} \\ \mathbf{0} & \mathbf{T}_b \end{bmatrix},\ \mathbf{T}_2 = \begin{bmatrix} \mathbf{T}_m & \mathbf{0} \\ \mathbf{0} & \mathbf{T}_m \end{bmatrix},$$

$$\mathbf{T}_b = \begin{bmatrix} 1 & -a \\ 1 & b \end{bmatrix},\ \mathbf{T}_m = \begin{bmatrix} 1 & -c \\ 1 & d \end{bmatrix}.$$

Forces generated by identical radial magnetic bearing have the form:

$$\begin{aligned} &F_{ax} = k_i i_{ax} + k_s x_a,\ \ F_{bx} = k_i i_{bx} + k_s x_b, \\ &F_{ay} = k_i i_{ay} + k_s y_a,\ \ F_{by} = k_i i_{by} + k_s y_b. \end{aligned} \tag{11}$$

The Laplace transform was applied to the equations of motion expressed by bearing plane co-ordinates:

$$\begin{aligned} &\begin{bmatrix} B(s) & A(s) & 0 & 0 \\ -C(s) & D(s) & -\Omega G(s) & \Omega G(s) \\ 0 & 0 & B(s) & A(s) \\ \Omega G(s) & -\Omega G(s) & -C(s) & D(s) \end{bmatrix} \begin{bmatrix} x_a(s) \\ x_b(s) \\ y_a(s) \\ y_b(s) \end{bmatrix} = \\ &= \begin{bmatrix} k_i & k_i & 0 & 0 \\ -ak_i & bk_i & 0 & 0 \\ 0 & 0 & k_i & k_i \\ 0 & 0 & -ak_i & bk_i \end{bmatrix} \begin{bmatrix} i_{xa}(s) \\ i_{xb}(s) \\ i_{ya}(s) \\ i_{yb}(s) \end{bmatrix} \end{aligned} \tag{12}$$

where:

$$\begin{aligned} &A(s) = \frac{ma}{l}s^2 - k_s, \quad B(s) = \frac{mb}{l}s^2 - k_s, \\ &C(s) = \frac{I_x}{l}s^2 - ak_s, \quad D(s) = \frac{I_x}{l}s^2 - bk_s, \\ &G(s) = \frac{I_z}{l}s. \end{aligned} \tag{13}$$

From equations (10) the co-ordinates in measurement planes can be calculated: $\mathrm{p}_m = \mathrm{T}_2\mathrm{T}_1^{-1}\mathrm{p}_b$, what leads to the transformation in xz-plane:

$$\begin{bmatrix} x_a \\ x_b \end{bmatrix} = \begin{bmatrix} \dfrac{d+a}{d+c} & \dfrac{c-a}{d+c} \\ \dfrac{d-b}{d+c} & \dfrac{c+b}{d+c} \end{bmatrix} \begin{bmatrix} x_c \\ x_d \end{bmatrix} = \begin{bmatrix} t_{11} & t_{12} \\ t_{21} & t_{22} \end{bmatrix} \begin{bmatrix} x_c \\ x_d \end{bmatrix} \tag{14}$$

Identical transformation is in *yz*-plane. Plant (12) has four inputs and four outputs and is of 8-order against complex variable *s*. Taking into account two first equations of (12) and measurement coordinates in *xz*-plane we have:

$$\Delta\begin{bmatrix} t_{11} & t_{12} \\ t_{21} & t_{22} \end{bmatrix}\begin{bmatrix} x_c \\ x_d \end{bmatrix}= \\ =\Omega G\begin{bmatrix} -A & A \\ B & -B \end{bmatrix}\begin{bmatrix} t_{11} & t_{12} \\ t_{21} & t_{22} \end{bmatrix}\begin{bmatrix} y_c \\ y_d \end{bmatrix}+ \\ +k_i\begin{bmatrix} D+aA & D-bA \\ C-aB & C+bB \end{bmatrix}\begin{bmatrix} i_{xa} \\ i_{xb} \end{bmatrix} \tag{15a}$$

From two last equations of (12) and measurement coordinates in *yz*-plane there is:

$$\Delta\begin{bmatrix} t_{11} & t_{12} \\ t_{21} & t_{22} \end{bmatrix}\begin{bmatrix} y_c \\ y_d \end{bmatrix}= \\ =\Omega G\begin{bmatrix} A & -A \\ -B & B \end{bmatrix}\begin{bmatrix} t_{11} & t_{12} \\ t_{21} & t_{22} \end{bmatrix}\begin{bmatrix} x_c \\ x_d \end{bmatrix}+ \\ +k_i\begin{bmatrix} D+aA & D-bA \\ C-aB & C+bB \end{bmatrix}\begin{bmatrix} i_{ya} \\ i_{yb} \end{bmatrix} \tag{15b}$$

where:

$$\Delta = B(s)D(s)+C(s)A(s)= \\ =\frac{1}{l}\left\{mI_x s^4-[2I_x+m(a^2+b^2)]k_s s^2+l^2 k_s{}^2\right\} \tag{16}$$

is characteristic polynomial of each subsystem. The variable *s* is omitted in above submodels.

3.1. PD controllers for the subsystems

For the control purposes we use the scheme from Figure 2 where the forces are summed. The control law for local loops (from Fig. 2a) is:

$$\begin{bmatrix} i_{xa}(s) \\ i_{xb}(s) \end{bmatrix}=-\begin{bmatrix} R_a(s) & 0 \\ 0 & R_b(s) \end{bmatrix}\begin{bmatrix} x_c(s) \\ x_d(s) \end{bmatrix} \tag{17}$$

where: $R_a(s)=k_{da}s+k_{pa}$, $R_b(s)=k_{db}s+k_{pb}$.

Similar control law can be defined for subsystem from Figure 2b. The control is realized in bearing planes while measurement is realized in sensor planes (non-collocated system). For collocated system the stability and proper quality is available for the following controller parameters (Gosiewski 2004):

$$k_p=k_{pa}=k_{pb}=1.5k_s/k_i,\ \ k_d=k_{da}=k_{db}=0.001k_p.$$

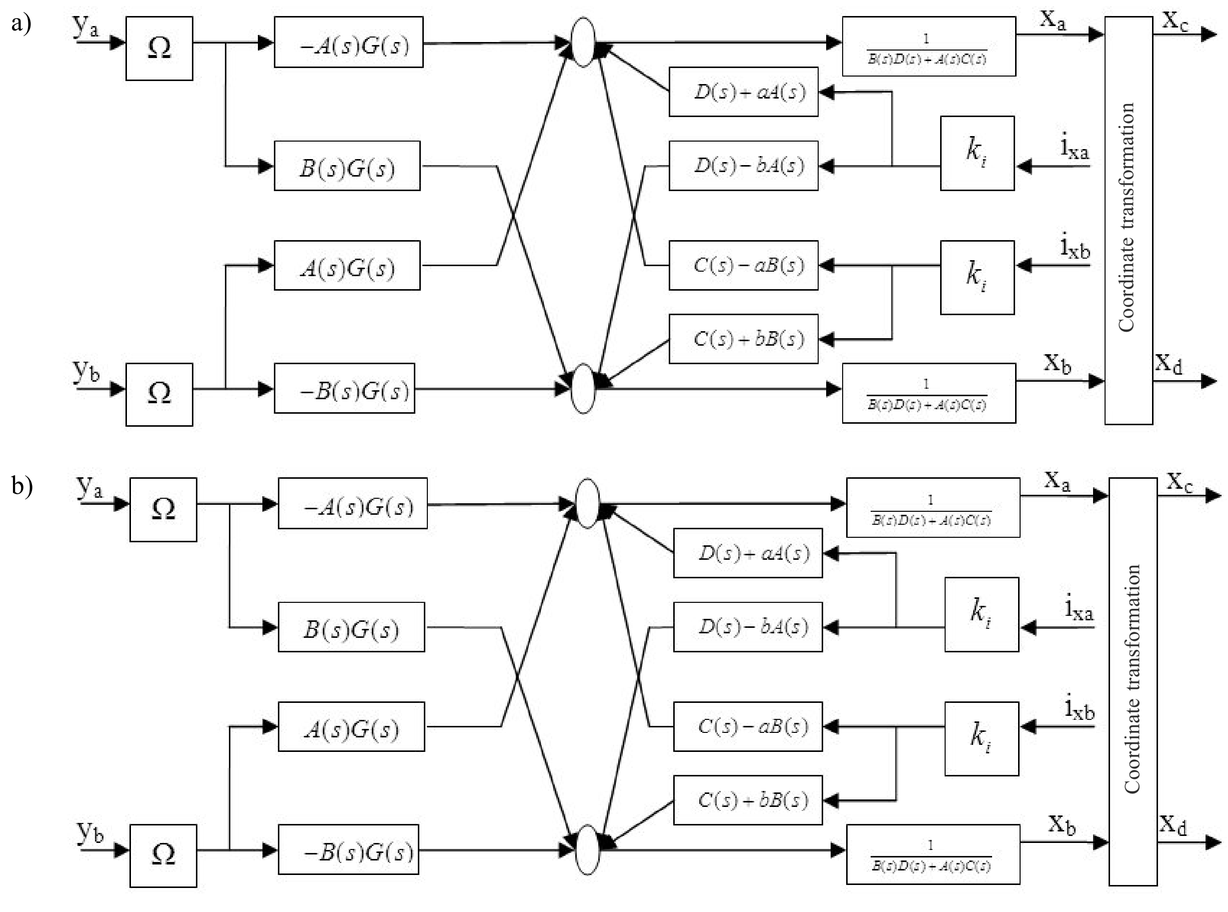

Fig. 2. Subsystems of the magnetically supported rigid rotor which present couplings between planes: a) from *yz*-plane to *xz*-plane; b) from xz-plane to yz-plane

The closed-loop subsystem from Figure 2a with two local PD controllers is described by matrix equation:

$$\begin{bmatrix} x_c \\ x_d \end{bmatrix} = \frac{\Omega G}{\Delta_z} \begin{bmatrix} G_{aai} & -G_{abi} \\ -G_{bai} & G_{bbi} \end{bmatrix} \begin{bmatrix} -A & A \\ B & -B \end{bmatrix} \begin{bmatrix} y_a \\ y_b \end{bmatrix} \tag{18}$$

where:

$$\begin{aligned} &G_{aai} = t_{22}\Delta + k_i(C+bB)R_b, \\ &G_{abi} = t_{12}\Delta + k_i(D-bA)R_b, \\ &G_{bai} = t_{21}\Delta + k_i(C-aB)R_a, \\ &G_{bbi} = t_{11}\Delta + k_i(D+aA)R_a, \\ &\Delta_z = \left[t_{11}\Delta + k_i(D+aA)R_a\right]\left[t_{22}\Delta + k_i(C+bB)R_b\right] + \\ &-\left[t_{21}\Delta + k_i(C-aB)R_a\right]\left[t_{12}\Delta + k_i(D+bA)R_b\right], \\ &\Delta = BD + CA. \end{aligned} \tag{18a}$$

Finally, the matrix multiplying in (18) leads to closed-loop subsystem in *xz*-plane:

$$\begin{bmatrix} x_c \\ x_d \end{bmatrix} = \\ = \frac{\Omega G}{\Delta_z} \begin{bmatrix} -(G_{aai}A + G_{abi}B) & G_{aai}A + G_{abi}B \\ G_{bai}A + G_{bbi}B & -(G_{bai}A + G_{bbi}B) \end{bmatrix} \begin{bmatrix} y_a \\ y_b \end{bmatrix} \tag{19}$$

In *yz*-plane the above relations are as follows:

$$\begin{bmatrix} y_a \\ y_b \end{bmatrix} = \\ = \frac{\Omega G}{\Delta_z} \begin{bmatrix} (G_{aai}A + G_{abi}B) & -(G_{aai}A + G_{abi}B) \\ -(G_{bai}A + G_{bbi}B) & (G_{bai}A + G_{bbi}B) \end{bmatrix} \begin{bmatrix} x_a \\ x_b \end{bmatrix} \tag{20}$$

After calculations of numerator and denominators in (19) and (20) we have:

$$\begin{aligned} &\begin{bmatrix} x_c \\ x_d \end{bmatrix} = \\ &= \frac{(d+c)\Omega G}{\Delta_z} \begin{bmatrix} -\Delta(t_{22}A + t_{12}B + k_iR_b) & \Delta(t_{22}A + t_{12}B + k_iR_b) \\ \Delta(t_{21}A + t_{11}B + k_iR_a) & -\Delta(t_{21}A + t_{11}B + k_iR_a) \end{bmatrix} \begin{bmatrix} y_a \\ y_b \end{bmatrix}, \\ &\begin{bmatrix} y_c \\ y_d \end{bmatrix} = \\ &= \frac{(d+c)\Omega G}{\Delta_z} \begin{bmatrix} \Delta(t_{22}A + t_{12}B + k_iR_b) & -\Delta(t_{22}A + t_{12}B + k_iR_b) \\ -\Delta(t_{21}A + t_{11}B + k_iR_a) & \Delta(t_{21}A + t_{11}B + k_iR_a) \end{bmatrix} \begin{bmatrix} x_a \\ x_b \end{bmatrix}, \end{aligned} \tag{21}$$

where:

$$\Delta_z = \Delta\Delta_{zm} = \\ = \Delta \left\{ \begin{aligned} &(t_{11}t_{22} - t_{12}t_{21})\Delta + k_i\left[t_{11}(C+bB) - t_{21}(D-bA)\right]R_b + \\ &\qquad + k_i\left[t_{22}(D+aA) - t_{12}(C-aB)\right]R_a + k_i^2 lR_aR_b \end{aligned} \right\}.$$

The minimal realization of transfer functions is obtained after removing of open-loop characteristic polynomial Δ:

$$\begin{aligned} &\begin{bmatrix} x_c(s) \\ x_d(s) \end{bmatrix} = \frac{\Omega G(s)}{\Delta_{zm}(s)} \begin{bmatrix} -D_1(s) & D_1(s) \\ D_2(s) & -D_2(s) \end{bmatrix} \begin{bmatrix} y_a(s) \\ y_b(s) \end{bmatrix}, \\ &\begin{bmatrix} y_c(s) \\ y_d(s) \end{bmatrix} = \frac{\Omega G(s)}{\Delta_{zm}(s)} \begin{bmatrix} D_1(s) & -D_1(s) \\ -D_2(s) & D_2(s) \end{bmatrix} \begin{bmatrix} x_a(s) \\ x_b(s) \end{bmatrix}. \end{aligned} \tag{22}$$

where:

$$\begin{aligned} &\Delta_{zm}(s) = (a+b)\Delta + k_i\left[(I_x + mac)s^2 - (c+b)lk_s\right]R_a + \\ &+ k_i\left[(I_x + mbd)s^2 - (a+d)lk_s\right]R_b + (d+c)k_i^2R_aR_bl, \\ &D_1(s) = mcs^2 + (-2c + a - b)k_s + (d+c)k_iR_b, \\ &D_2(s) = mds^2 + (-2d - a + b)k_s + (d+c)k_iR_a. \end{aligned} \tag{23}$$

Transfer function matrices in *xz*- and *yz*-planes differ only by sign. $\Delta_{zm} = 0$ is a characteristic equation in both subsystems.

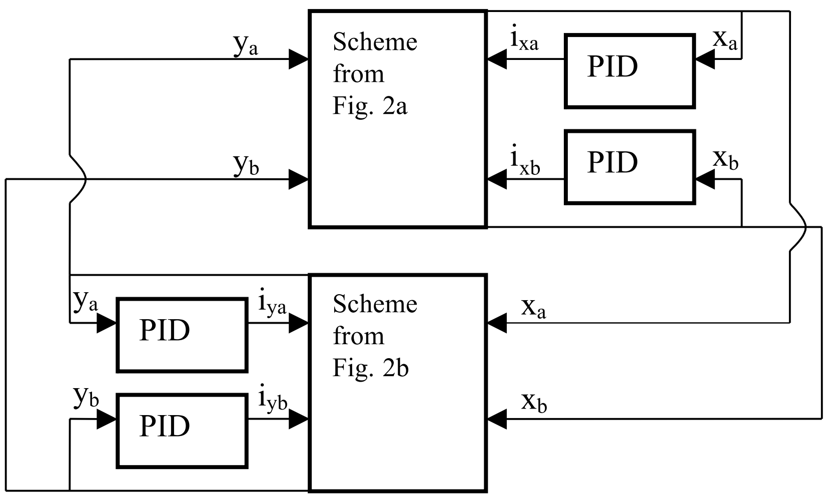

Fig. 3. Scheme of full closed-loop system with local PID controllers

3.2. Recollocation of sensors and actuators signals

The subsystems described by equations should be connected to design the full closed-loop system in the form shown in Figure 4. So more, it is well known (Preumont 2002), that non-collocation of sensor and actuator planes deteriorate the system dynamics. Non-collocation can leads to the non-minimumphase of the control plant because zeros of transfer functions move to the right halfplane of the variable s. Much better case is when the sensors and actuators are collocated. In some cases we are able to estimate the displacement of the coordinates in actuator planes by the displacements measured in sensor planes and vice versa (Gosiewski *et al*. 2010). In motion equations we compare forces or momentum of forces. So more, in case of local control loops we design the feedback and generate the control forces in the actuator planes. Therefore, it is useful to estimate the displacements in the magnetic bearing planes. To transfer the sensor plane displacements $x_c(s)$, $x_d(s)$ to the actuator plane displacements $x_a(s)$, $x_b(s)$ the equations (10) are used again:

$$\mathbf{p}_m = \mathbf{T}_2\mathbf{T}_1^{-1}\mathbf{p}_b = \mathbf{P}\mathbf{p}_b \tag{24}$$

what in xz-plane leads to the transformation:

$$\begin{bmatrix} y_c \\ y_d \end{bmatrix} = \begin{bmatrix} \frac{b+c}{b+a} & \frac{a-c}{b+a} \\ \frac{b-d}{b+a} & \frac{a+d}{b+a} \end{bmatrix} \begin{bmatrix} y_a \\ y_b \end{bmatrix} = \begin{bmatrix} p_{11} & p_{12} \\ p_{21} & p_{22} \end{bmatrix} \begin{bmatrix} y_a \\ y_b \end{bmatrix}. \tag{25}$$

The control law can be presented in the form:

$$\begin{bmatrix} i_{xa}(s) \\ i_{xb}(s) \end{bmatrix} = -\begin{bmatrix} R_a(s) & 0 \\ 0 & R_b(s) \end{bmatrix} \begin{bmatrix} p_{11} & p_{12} \\ p_{21} & p_{22} \end{bmatrix} \begin{bmatrix} x_a(s) \\ x_b(s) \end{bmatrix}. \tag{26}$$

But it is much more conveniently to transform the measured signals in the way shown in Figure 4.

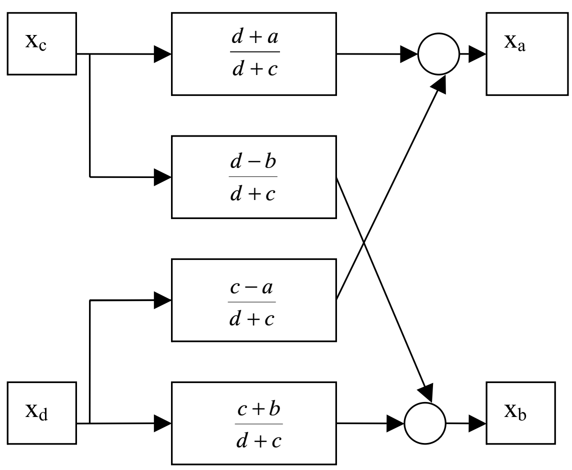

Fig. 4. Transformation of the measured signals

Such calculations (Fig. 4) in case of rigid rotor are sufficient to change the non-collocated system into collocated one.

3.3. Full closed-loop system

The full system have four inputs and four outputs as it is shown in Figure 5.

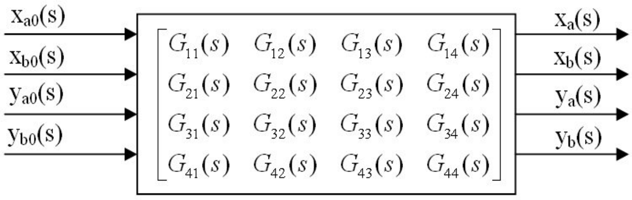

Fig. 5. Full closed-loop system

Taking into account considerations from above chapters it can be replaced by two-input two output transfer functions. To obtain the full system the models (22) are joined into one closed-loop system as it is shown in Figure 6.

We break the feedback loop in the place indicated by tildes to obtain open-loop system. The open-loop transfer function is obtained by the multiplication of matrices:

$$\mathbf{H}_o = \begin{bmatrix} -H_1(s) & H_1(s) \\ H_2(s) & -H_2(s) \end{bmatrix}, \tag{27}$$

where:

$$H_1(s) = \frac{s^2\Omega^2G^2}{\Delta^2_{zmi}}\left[(sA + k_iL_b)^2 + (sA + k_iL_b)(sB + k_iL_a)\right],$$
$$H_2(s) = \frac{s^2\Omega^2G^2}{\Delta^2_{zmi}}\left[(sB + k_iL_a)(sA + k_iL_b) + (sB + k_iL_a)^2\right]. \tag{28}$$

The closed-loop system, according to Figure (7a) is as follows:

$$\begin{bmatrix} x_a(s) \\ x_b(s) \end{bmatrix} = \begin{bmatrix} -H_1(s) & H_1(s) \\ H_2(s) & -H_2(s) \end{bmatrix} \begin{bmatrix} x_a(s) + x_{a0}(s) \\ x_b(s) + x_{b0}(s) \end{bmatrix}, \tag{29}$$

After some calculations we have:

$$\left\{\begin{bmatrix} 1 & 0 \\ 0 & 1 \end{bmatrix} - \begin{bmatrix} -H_1 & H_1 \\ H_2 & -H_2 \end{bmatrix}\right\} \begin{bmatrix} x_a \\ x_b \end{bmatrix} = \begin{bmatrix} -H_1 & H_1 \\ H_2 & -H_2 \end{bmatrix} \begin{bmatrix} x_{a0} \\ x_{b0} \end{bmatrix},$$

and

$$\begin{bmatrix} x_a \\ x_b \end{bmatrix} = \frac{1}{\Delta_{zci}} \begin{bmatrix} 1+H_2 & H_1 \\ H_2 & 1+H_1 \end{bmatrix} \begin{bmatrix} -H_1 & H_1 \\ H_2 & -H_2 \end{bmatrix} \begin{bmatrix} x_{a0} \\ x_{b0} \end{bmatrix}, \tag{30}$$

where:

$$\Delta_{zci} = (1 + H_2)(1 + H_1) - H_1H_2 = 1 + H_1 + H_2, \tag{31}$$

is a characteristic polynomial. Finally, input/output relations are as follows:

$$\begin{bmatrix} x_a \\ x_b \end{bmatrix} = \frac{1}{1+H_1+H_2}\begin{bmatrix} -H_1 & H_1 \\ H_2 & -H_2 \end{bmatrix}\begin{bmatrix} x_{a0} \\ x_{b0} \end{bmatrix}, \tag{32}$$

Above relations can be expressed by transfer functions (28). In this case the characteristic polynomial is as follows:

$$\Delta_{zci} = \frac{\left\{\Delta^2{}_{zmi} + s^2\Omega^2G^2\left[(sA+k_iL_b)+(sB+k_iL_a)\right]^2\right\}}{\Delta^2{}_{zmi}} \tag{33}$$

and the input/output relation in the following form:

$$\begin{bmatrix} x_a \\ x_b \end{bmatrix} = \begin{bmatrix} \dfrac{-s^2\Omega^2G^2\left[(sA+k_iL_b)^2+(sB+k_iL_a)(sA+k_iL_b)\right]}{\Delta^2{}_{zm}+s^2\Omega^2G^2\left[(sA+k_iL_b)+(sB+k_iL_a)\right]^2} & \dfrac{s^2\Omega^2G^2\left[(sA+k_iL_b)^2+(sB+k_iL_a)(sA+k_iL_b)\right]}{\Delta^2{}_{zm}+s^2\Omega^2G^2\left[(sA+k_iL_b)+(sB+k_iL_a)\right]^2} \\ \dfrac{s^2\Omega^2G^2\left[(B+k_iL_a)(A+k_iL_b)+(B+k_iL_a)^2\right]}{\Delta^2{}_{zm}+s^2\Omega^2G^2\left[(A+k_iL_b)+(B+k_iL_a)\right]^2} & \dfrac{-s^2\Omega^2G^2\left[(sB+k_iL_a)(sA+k_iL_b)+(sB+k_iL_a)^2\right]}{\Delta^2{}_{zm}+s^2\Omega^2G^2\left[(sA+k_iL_b)+(sB+k_iL_a)\right]^2} \end{bmatrix}\begin{bmatrix} x_{a0} \\ x_{b0} \end{bmatrix} \tag{34}$$

It is evident from above transfer functions, that the closed loop system is of 8-order and equation (34) is minimal realization of system.

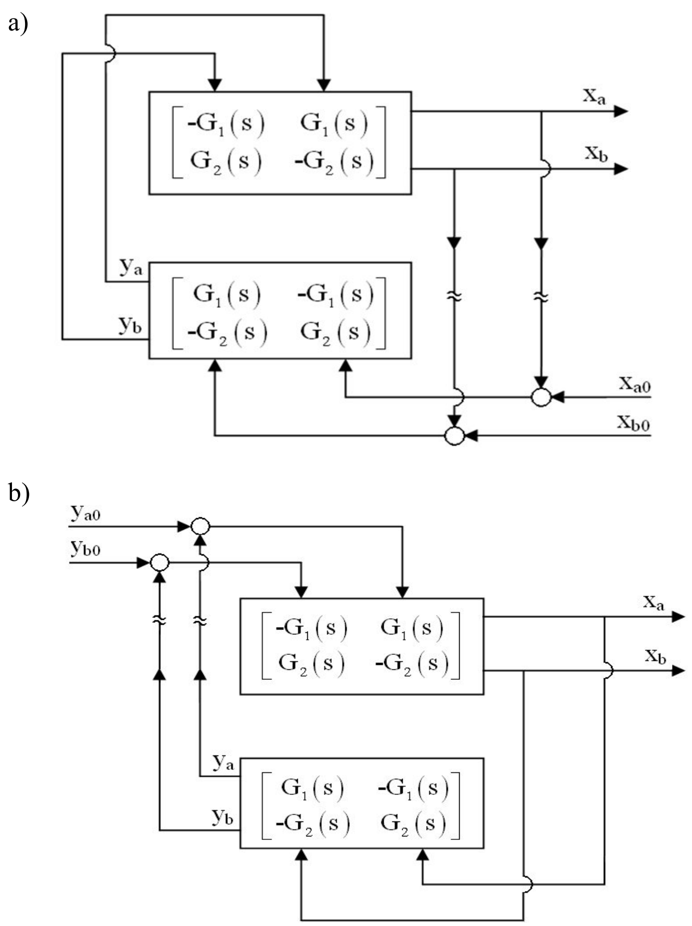

Fig. 6. Open-loop and closed-loop system in decoupled form for a) inputs and outputs in *xz*-plane (first quarter in matrix from Fig. 5); b) inputs and outputs in *yz*-plane (fourth quarter in matrix from Fig. 5)

3.4. Stability

Full closed-loop subsystem will be stable when real parts of poles will be negative. According to equations (23) the characteristic equation of the closed-loop subsystem has the form:

$$\Delta_{zm} = (a+b)\frac{1}{l}\left\{mI_x s^4 - [2I_x + m(a^2+b^2)]k_s s^2 + l^2 k_s{}^2\right\} +$$
$$+k_i\left[(I_x + mac)s^2 - (c+b)lk_s\right](k_{da}s + k_{pa}) +$$
$$+k_i\left[(I_x + mbd)s^2 - (d+a)lk_s\right](k_{db}s + k_{pb}) +$$
$$+(d+c)k_i^2(k_{da}s + k_{pa})(k_{db}s + k_{pb})l.$$

The characteristic equation can be written in short form:

$$\Delta_{zm} = a_4 s^4 + a_3 s^3 + a_2 s^2 + a_1 s + a_0 = 0 \tag{35}$$

where:

$$\begin{aligned} a_4 &= mI_x, \\ a_3 &= k_i(I_x + mac)k_{da} + k_i(I_x + mbd)k_{db}, \\ a_2 &= -[2I_x + m(a^2+b^2)]k_s + k_i(I_x + mac)k_{pa} + \\ &\quad + k_i(I_x + mbd)k_{pb} + (d+c)k_i^2 k_{da}k_{db}l, \\ a_1 &= -k_i(c+b)lk_s k_{da} - k_i(d+a)lk_s k_{db} + \\ &\quad + (d+c)k_i^2(k_{da}k_{pb} + k_{db}k_{pa})l, \\ a_0 &= l^2 k_s{}^2 - k_i(c+b)lk_s k_{pa} - k_i(d+a)lk_s k_{pb} + \\ &\quad + (d+c)k_i^2 k_{pa}k_{pb}l. \end{aligned} \tag{36}$$

Collocated system

In case of collocated sensors and actuators when: $c = a$, $d = b$ there is:

$$\begin{aligned} a_4 &= mI_x, \\ a_3 &= k_i\left(I_x + ma^2\right)k_{da} + k_i\left(I_x + mb^2\right)k_{db}, \\ a_2 &= -[2I_x + m(a^2+b^2)]k_s + k_i\left(I_x + ma^2\right)k_{pa} + \\ &\quad + k_i\left(I_x + mb^2\right)k_{pb} + k_i^2 k_{da}k_{db}l^2, \\ a_1 &= -k_i l^2 k_s(k_{db} + k_{da}) + k_i^2(k_{da}k_{pb} + k_{pa}k_{db})l^2, \\ a_0 &= l^2 k_s{}^2 - k_i l^2 k_s(k_{pb} + k_{pa}) + k_i^2 k_{pa}k_{pb}l^2. \end{aligned} \tag{37}$$

For identical control laws $k_p = k_{pa} = k_{pb}$, $k_d = k_{da} = k_{db}$ from necessary conditions of Hurwitz criterion it results that system is stable for controller parameters: $k_p > k_s / k_i$; $k_d > 0$. To achive good performace of the closed-loop system the PD-controller parameters were chosen as: $k_p = 1.5k_s / k_i$, $k_d = 0.001k_p$. The sufficient conditions of Hurwitz criterion leads to inequilitys: $a_3a_2 - a_1a_4 > 0$, $a_3a_2a_1 - a_3^2a_0 - a_1^2a_4 > 0$, which are fulfilled for collocated system.

The stability analysis for full closed-loop system can be carried out by solving of the characteristic equation:

$$\begin{aligned} \Delta_{zc} &= \left|\mathbf{I} + \mathbf{H_o}\right| = \\ &= \Delta^2{}_{zm} + \Omega^2 G^2\left[(A + k_iR_b) + (B + k_iR_a)\right]^2 = 0 \end{aligned} \tag{38}$$

To do his the root locus method will be used. The rotor angular speed K = Ω^2 can be considered as an Evans gain. The characteristic equation (38) is presented in the form:

$$1 + KG_o(s) = 0, \tag{39}$$

where:

$$G_o(s) = \frac{G^2\left[(A + k_iR_b) + (B + k_iR_a)\right]^2}{\Delta^2{}_{zm}}, \tag{40}$$

is a model of a SISO system. For such system we can use root locus metod or Nyquist criteron to check the system stability.

Non-collocated system

The investigations will be carried out for noncollocated system when the right sensor moves away from the right bearing support. In that case there is: $c = a$, $d = b + \delta$ and coefficients of the characteristic equation are in the form:

$$\begin{aligned} a_4 &= mI_x, \\ a_3 &= k_i(I_x + ma^2)k_{da} + k_i(I_x + mb(b+\delta)k_{db}, \\ a_2 &= -[2I_x + m(a^2+b^2)]k_s + k_i(I_x + ma^2)k_{pa} + \\ &\quad + k_i(I_x + mb(b+\delta))k_{pb} + (b+a+\delta)k_i^2 k_{da}k_{db}l, \\ a_1 &= -k_i l^2 k_s k_{da} - k_i(l+\delta)lk_s k_{db} + \\ &\quad + (l+\delta)k_i^2(k_{da}k_{pb} + k_{db}k_{pa})l, \\ a_0 &= l^2 k_s{}^2 - k_i l^2 k_s k_{pa} - k_i(l+\delta)lk_s k_{pb} + \\ &\quad + (l+\delta)k_i^2 k_{pa}k_{pb}l. \end{aligned} \tag{41}$$

When sensor plane moves away the characteristic equation can be put in the following form:

$$\Delta_{zm} = \Delta' + \delta\Delta'' = 0,$$
$$\Delta' = a'_4 s^4 + a'_3 s^3 + a'_2 s^2 + a'_1 s + a'_0 = 0, \quad (42)$$
$$\Delta'' = a''_3 s^3 + a''_2 s^2 + a''_1 s + a''_0 = 0.$$

The polynomial Δ' is identical with characteristic polynomial of collocated system (37) while polynomial Δ'' has the following coefficients:

$$a''_3 = k_i mbk_{db},$$
$$a''_2 = k_i mbk_{pb} + k_i^2 k_{da} k_{db} l,$$
$$a''_1 = -k_i lk_s k_{db} + k_i^2 (k_{da} k_{pb} + k_{db} k_{pa}) l, \quad (43)$$
$$a''_0 = -k_i lk_s k_{pb} + k_i^2 k_{pa} k_{pb} l.$$

Eq. (42) for increasing δ (sensor plane moves away on the right – positive direction of axies *z*) can be presented in the form:

$$\Delta_{zm} = 1 + \delta \frac{\Delta''}{\Delta'} = 0, \quad (44)$$

while for decreasing δ (sensor plane moves away on the left – negative direction of axies *z*) in the following form:

$$\Delta_{zm} = 1 - \delta \frac{\Delta''}{\Delta'} = 0. \quad (45)$$

Such presentation of characteristic equations simplifies the analysis of the sensor location influence on system stability.

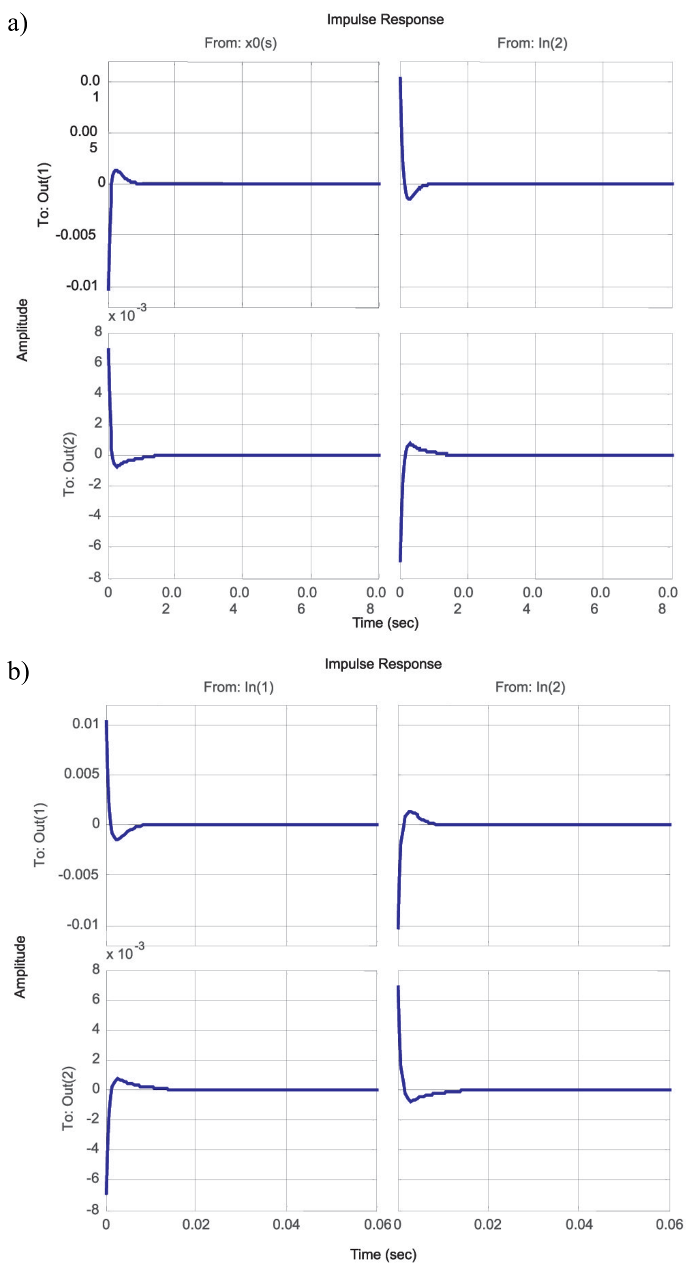

Fig. 7. Impulse responses of: a) subsystem *xz*; b) subsystem *yz*

3.5. Numerical simulations

The computer simulations were carried out for the following rotor and bearing parameters: m = 18.5 [kg], J_z = 0.0115 [kgm^2], k_s = 1.6024e + 06 [N/m], k_i = 100.1483 [A/m], l = 0.902 m, a = 0.6l, b = l–a. Axial moment of inertia was: J_{x1} = 0.6525 [kgm^2].

A computer simulations were be carried out for collocated and for non-collocated systems with local PD-controllers.

Collocated system

Both control laws have the same coefficients: k_P = = 2.4e + 04 [N/A], k_D = 24 [Ns/m]. The impulse responses are stable as we can see in Figure 7. All Hurwitz conditions are fulfilled what confirms the subsystems stability for slowly rotating rotor. To check stability of the full system the real and imaginary parts of the characteristic polynomial roots were carried out for rotor angular speeds in the range from 0 to 3000 [rad/s] (0–31400 [rpm]), and results are shown in Figure 8.

The obtained results were confirmed by root locus method for system (34) with Evans gain K = Ω^2 and are presented in Figure 9. The full closed-loop system with local PD-controllers is stable for all rotor angular speeds Ω.

The impulse responses of full closed-loop system were checked for rotor angular speed Ω = 3000 [rad/s]. Since the both subsystems are screw-symmetric only response for inputs/outputs in *xz*-plane are presented in Figure 10.

The gyroscopic effect increases values of responses but system is stable.

Non-collocated system

In considered non-collocated case the right sensor plane moves away from the right control plane. The distance of the sensor plane from mass centre is $d = b + \delta$ where b = 0.36 [m]. We are looking for value of δ when system is on the stability order. For the movement in right direction the formula (44) is used to employ the root locus method. For non-rotating rotor the results are shown in Figure 11. For any δ the system is stable.

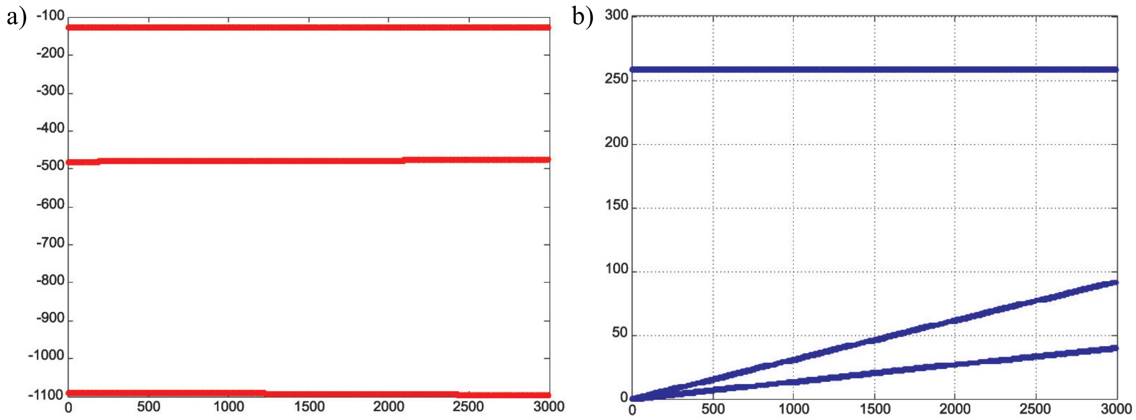

Fig. 8. Real (a) and imaginary (b) parts of full closed-loop system poles in the range Ω = 0÷3000 [rad/s]

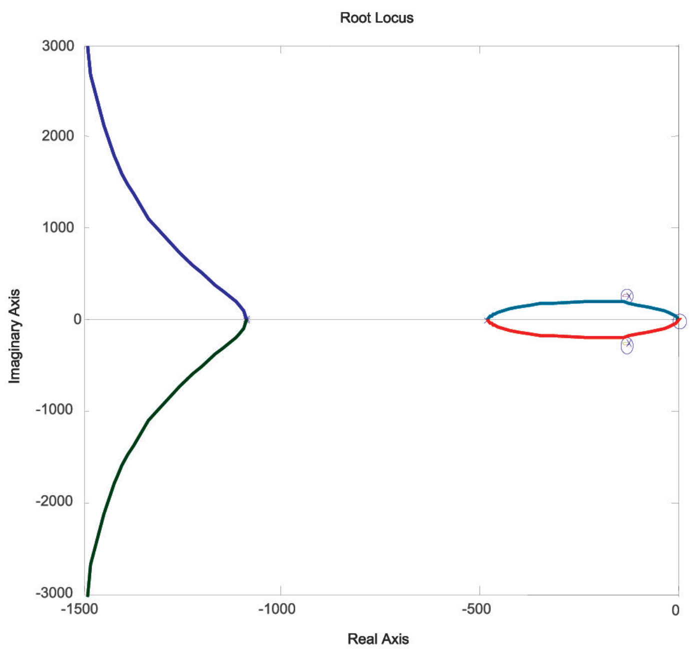

Fig. 9. Root lines of the full system with rotor angular speed Ω^2 as an Evans gain

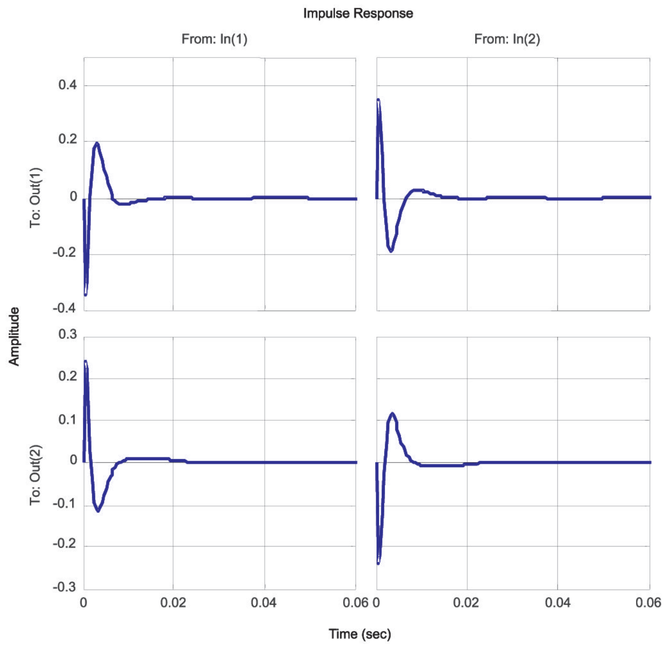

Fig. 10. Impulse responses of closed-loop system in *xz*-plane excited also in *xz*-plane for angular speed: Ω = 3000 [rad/s]

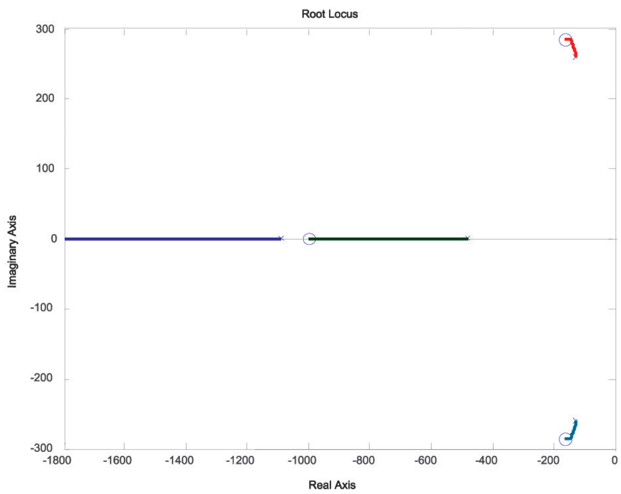

Fig. 11. Root locus of the closed-loop system with non-rotating rotor when distance δ moves away on the right

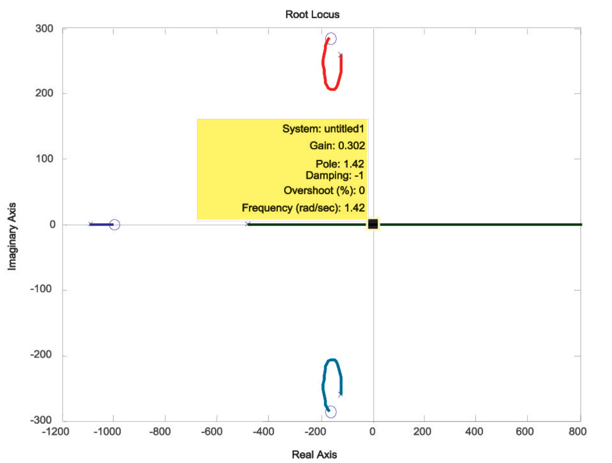

Fig. 12. Root locus of the closed-loop system with non-rotating rotor when distance δ moves away on the left (in the nodal point direction)

Now, the sensor planes is moved no the left from control plane and distance of the sensor plane from rotor mass centre is: $d = b - \delta$. The stability border will be found from formula (45). For non-rotating rotor the results are shown in Figure 12. In the text box there is given the distance δ = 0.302 [m] on the stability border. The instability results from the fact that sensor approach the nodel point of rotational mode which is in the mass centre.

Next, the influence of rotor rotation on the stability of full system was checked for two locations of the sensor plane: $d = 0.16$ [m] (δ = 0.2 [m] – Fig. 13) and $d = -0.04$ [m] (δ = 0.4 [m] – Fig. 14).

The sign minus means that sensor plane is at opposite side of the rotor mass centre (nodal point) than the control plane.

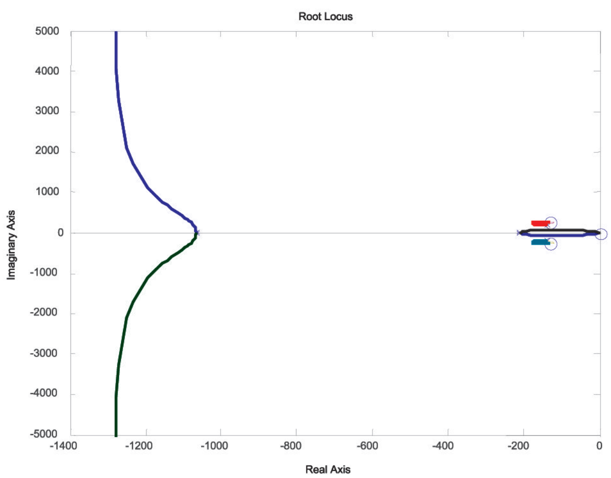

Fig. 13. Root locus for Evans gain Ω^2 and constant sensor plane distance δ = 0.2 [m]($d = 0.16$ [m])

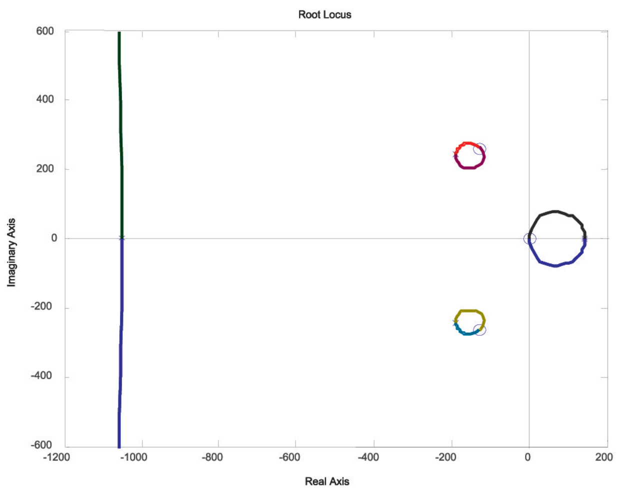

Fig. 14. Root locus for Evans gain Ω^2 and constant sensor plane distance $\delta = 0.4$ [m]($d = -0.04$ [m])

From Figures 12–14 it results that in case of non-collocated rotating system with PD-controllers the stability depends on the sensor and actuator location and not on rotor angular speeds. The opposite location of sensor and actuators against nodal points is the simplest way to obtain unstable closed-loop system.

4. THE CONCEPT OF THE GENERAL RECOLLOCATION METHOD

4.1. State-space models and their transformations

Using the state-space approach the control plant can be described by the following state (46) and output (47) equations

$$\dot{\mathbf{x}}(t) = \mathbf{A}\mathbf{x}(t) + \mathbf{B}\mathbf{u}(t) \quad (46)$$

$$\mathbf{y}(t) = \mathbf{C}\mathbf{x}(t) + \mathbf{D}\mathbf{u}(t) \quad (47)$$

with state matrix $\mathbf{A}$ [$n\times n$], input (control) matrix $\mathbf{B}$ [$n\times m$], output (measurement) matrix $\mathbf{C}$ [$m\times n$] and, feedthrough matrix $\mathbf{D}$ [$m\times m$]. Note, that the number of inputs $\mathbf{u}(t)$ equals the number of outputs $\mathbf{y}(t)$ here. In such case local control loops with one input and one output can be used. When the similarity transformation is applied matrix $\mathbf{D}$ does not change, as it is input/output invariant. That is why the output equation can be reduced to the following form

$$\mathbf{y}(t) = \mathbf{C}\mathbf{x}(t) \quad (48)$$

We will assume, that pair ($\mathbf{A}$, $\mathbf{C}$) is observable i.e., the rank of observability matrix $\mathbf{S}_o$ equals n, where n is the length of state vector $\mathbf{x}(t)$ and, $\mathbf{S}_o = [\mathbf{C}, \mathbf{CA}, \mathbf{CA}^2, \ldots, \mathbf{CA}^{n-1}]^T$. The state vector can be transformed as follows

$$\mathbf{x}_o(t) = \mathbf{T}_o\mathbf{x}(t) \quad (49a)$$

or

$$\mathbf{x}_o(t) = \mathbf{T}_o^{-1}\mathbf{x}(t) \quad (49b)$$

where $\mathbf{T}_o^{-1}$ is the matrix transforming $\mathbf{A}$ to $\mathbf{A}_o$ by similarity and, $\mathbf{x}_o(t)$ is the vector of observable states. The above dependencies yield, that transformation matrix $\mathbf{T}_o$ is not singular. Its rows are the rows of the observability matrix $\mathbf{S}_o$ and are constructed according to the Luenberger-Brunowski theorem (Kaczorek 1983). Introducing transformation (49) into system (46), (48), yields

$$\mathbf{T}_o^{-1}\dot{\mathbf{x}}_o(t) = \mathbf{A}\mathbf{T}_o^{-1}\mathbf{x}_o(t) + \mathbf{B}\mathbf{u}(t) \quad (50)$$

$$\mathbf{y}(t) = \mathbf{C}\mathbf{T}_o^{-1}\mathbf{x}_o(t) \quad (51)$$

Multiplying by $\mathbf{T}_o$ system (46), (48) can be transformed to the following observable canonical form

$$\dot{\mathbf{x}}_o(t) = \mathbf{A}_o\mathbf{x}_o(t) + \mathbf{B}_o\mathbf{u}(t) \quad (52)$$

$$\mathbf{y}(t) = \mathbf{C}_o\mathbf{x}_o(t) \quad (53)$$

where $\mathbf{A}_o = \mathbf{T}_o\mathbf{A}\mathbf{T}_o^{-1}, \mathbf{B}_o = \mathbf{T}_o\mathbf{B}, \mathbf{C}_o = \mathbf{C}\mathbf{T}_o^{-1}$. The similarity of state matrices $\mathbf{A}$ and $\mathbf{A}_o$ is conditioned by the equality of the characteristic polynomials

$$\det[s\mathbf{I} - \mathbf{A}] = \det[s\mathbf{I} - \mathbf{A}_o] \quad (54)$$

In general the elements of matrix $\mathbf{C}_o$ are ones or zeros but, in some particular case they can be grouped in such a way, that

$$\mathbf{C}_o = \mathbf{C}\mathbf{T}_o = [\mathbf{I} \,\vdots\, \mathbf{0}] \quad (55)$$

with unity matrix $\mathbf{I}$ [$m\times m$] and zero matrix $\mathbf{0}$ [$m\times(n-m)$]. Such canonical forms are discussed in the present paper.

Furthermore, we will assume that pair ($\mathbf{A}$, $\mathbf{B}$) is controllable i.e., the rank of controllability matrix $\mathbf{S}_s$ also equals n, where n is the length of state vector $\mathbf{x}(t)$ and, $\mathbf{S}_s = [\mathbf{B}, \mathbf{AB}, \mathbf{A}^2\mathbf{B}, \ldots, \mathbf{A}^{n-1}\mathbf{B}]$. The state vector can be transformed as follows

$$\mathbf{x}(t) = \mathbf{T}_s\mathbf{x}_s(t) \quad (56)$$

what yields the following controllable canonical form

$$\dot{\mathbf{x}}_s(t) = \mathbf{A}_s\mathbf{x}_s(t) + \mathbf{B}_s\mathbf{u}(t) \quad (57)$$

$$\mathbf{y}(t) = \mathbf{C}_s\mathbf{x}_s(t) \quad (58)$$

where $\mathbf{A}_s = \mathbf{T}_s^{-1}\mathbf{A}\mathbf{T}_s, \mathbf{B}_s = \mathbf{T}_s^{-1}\mathbf{B}, \mathbf{C}_s = \mathbf{C}\mathbf{T}_s$. Matrix $\mathbf{T}_s$ is not singular and its columns are the columns of controllability matrix $\mathbf{S}_s$ and are constructed according to the

Luenberger-Brunowski theorem (Kaczorek 1983). In a particular case input matrix $\mathbf{B}_s$ can have the following form

$$\mathbf{B}_s = \begin{bmatrix} \mathbf{I} \\ \cdots \\ \mathbf{0} \end{bmatrix} \tag{59}$$

The recollocated system with the measurements taken at the locations of the control actuators should have the following form

$$\dot{\mathbf{x}}(t) = \mathbf{A}\mathbf{x}(t) + \mathbf{B}\mathbf{u}(t) \tag{60}$$

$$\mathbf{z}(t) = \mathbf{B}_{\mathbf{C}}^{T}\mathbf{x}(t) \tag{61}$$

Superscript T of matrix $\mathbf{B}_{\mathbf{C}}^{T}$ denotes that its dimensions are of transposed matrix $\mathbf{B}$, while subscript $\mathbf{C}$ denotes that its elements are ones at the locations of the required axes/planes of actuation. We will assume that pair $(\mathbf{A}, \mathbf{B}_{\mathbf{C}}^{T})$ is observable i.e., the rank of observability matrix $\mathbf{S}_z$ is n, where n equals the length of state vector $\mathbf{x}(t)$ and, $\mathbf{S}_z = [\mathbf{B}_{\mathbf{C}}^{T}, \mathbf{B}_{\mathbf{C}}^{T}\mathbf{A}, \mathbf{B}_{\mathbf{C}}^{T}\mathbf{A}^2, \ldots, \mathbf{B}_{\mathbf{C}}^{T}\mathbf{A}^{n-1}]^T$. The observable canonical form can be obtained by the following transformation

$$\mathbf{x}(t) = \mathbf{T}_z^{-1}\mathbf{x}_z(t) \tag{62}$$

where $\mathbf{T}_z$ consists of the selected rows of observability matrix $\mathbf{S}_z$ (Kaczorek 1983). Applying transformation (62) the recollocated system can be presented as

$$\dot{\mathbf{x}}_z(t) = \mathbf{A}_z\mathbf{x}_z(t) + \mathbf{B}_z\mathbf{u}(t) \tag{63}$$

$$\mathbf{y}(t) = \mathbf{C}_z\mathbf{x}_z(t) \tag{64}$$

where: $\mathbf{A}_z = \mathbf{T}_z\mathbf{A}\mathbf{T}_z^{-1}, \mathbf{B}_z = \mathbf{T}_z\mathbf{B}, \mathbf{C}_z = \mathbf{B}_{\mathbf{C}}^{T}\mathbf{T}_z^{-1}$. Similarly to $\mathbf{C}_o$ matrix $\mathbf{C}_z$ can have the following particular form

$$\mathbf{C}_{\mathbf{z}} = \mathbf{B}_C^T\mathbf{T}_z^{-1} = [\mathbf{I} \vdots \mathbf{0}] \tag{65}$$

For orthogonal matrices $\mathbf{M}^T\mathbf{M} = \mathbf{M}\mathbf{M}^T = \mathbf{I}$ and, $\mathbf{M}^T = \mathbf{M}^{-1}$. Thus

$$\mathbf{x}_o(t) = \begin{bmatrix} \mathbf{y}(t) \\ \mathbf{x}_{o2}(t) \end{bmatrix}, \quad \mathbf{x}_z(t) = \begin{bmatrix} \mathbf{z}(t) \\ \mathbf{x}_{z2}(t) \end{bmatrix}, \tag{66}$$

where $\mathbf{x}_{o2}(t), \mathbf{x}_{z2}(t)$ are other unmeasured state variables. Inverse transformations $\mathbf{T}_o\mathbf{x}(t) = \mathbf{x}_o(t), \mathbf{T}_z\mathbf{x}(t) = \mathbf{x}_z(t)$ lead to

$$\begin{bmatrix} \mathbf{z}(t) \\ \mathbf{x}_{z2}(t) \end{bmatrix} = \mathbf{T}_z\mathbf{T}_o^{-1}\begin{bmatrix} \mathbf{y}(t) \\ \mathbf{x}_{o2}(t) \end{bmatrix} = \mathbf{P}_r\begin{bmatrix} \mathbf{y}(t) \\ \mathbf{x}_{o2}(t) \end{bmatrix}. \tag{67}$$

Thus state vector $\mathbf{x}(t)$ can be recollocated to required $\mathbf{z}(t)$ with the use of the proper submatrix of $\mathbf{P}_r = \mathbf{T}_z\mathbf{T}_o^{-1}$. The dimensions of this submatrix result from the length of $\mathbf{z}(t)$. Depending on the control method whole state vector $\mathbf{x}_z(t)$ or only reduced $\mathbf{z}(t)$ can be used.

In multidimensional vibration and motion control systems sensors of identical gains k_s and actuators of identical gains k_a are used most often. Moreover, if measured and actuated quantities depend closely on each other (e.g. measured – acceleration, actuated – force), transformation (67) can be simplified. Note, that

$$\mathbf{C}_z = \mathbf{B}_s^T. \tag{68}$$

what after applying $(\mathbf{M}\mathbf{N})^T = \mathbf{N}^T\mathbf{M}^T$ yields

$$\mathbf{B}_{\mathbf{C}}^{T}\mathbf{T}_z^{-1} = \mathbf{B}^T(\mathbf{T}_s^{-1})^T. \tag{69}$$

If sensors of identical gains k_s and actuators of identical gains k_a are applied, the following dependency becomes true

$$\frac{k_s}{k_a}\mathbf{B}^T\mathbf{T}_z^{-1} = \mathbf{B}^T(\mathbf{T}_s^{-1})^T,$$

what after introducing $(\mathbf{M}^T)^{-1} = (\mathbf{M}^{-1})^T$, yields

$$\frac{k_s}{k_a}\mathbf{T}_z^{-1} = (\mathbf{T}_s^{-1})^T = (\mathbf{T}_s^T)^{-1}, \tag{70}$$

and

$$\mathbf{T}_z = \frac{k_s}{k_a}\mathbf{T}_s^T. \tag{71}$$

Finally the following dependency can be obtained

$$\begin{bmatrix} \mathbf{z}(t) \\ \mathbf{x}_{z2}(t) \end{bmatrix} = \frac{k_s}{k_a}\mathbf{T}_s^T\mathbf{T}_o\begin{bmatrix} \mathbf{y}(t) \\ \mathbf{x}_{o2}(t) \end{bmatrix} = \mathbf{P}_r\begin{bmatrix} \mathbf{y}(t) \\ \mathbf{x}_{o2}(t) \end{bmatrix}. \tag{72}$$

Formulae (67) or (72) are the main result showing how to transform the given plant to its canonical forms and then to calculate virtual measurements at almost any point (given by selected elements of the state vector) using observable $\mathbf{T}_o$, controllable $\mathbf{T}_s$ and modified observable $\mathbf{T}_z$ transformation matrices. The matrices can be calculated based on the Luenberger-Brunowski theorem (Kaczorek 1983).

Providing that vector $\mathbf{y}$ in Eqs. (67) and (72) is measured, vector $\mathbf{x}_{o2}(t)$ should be estimated. For this reduced-order observer can be applied.

4.2. Reduced-order observer

Consider system (46), (48) and assume (not losing the generality of our discussion), that its m outputs are linearly independent or, what is equivalent, that the rank of matrix $\mathbf{C}$ is m. Then, matrix $\mathbf{C}$ can be transformed to

$\mathbf{C} = [\mathbf{I}_m \ \mathbf{0}_{m\times(n-m)}]$ i.e., partitioned into unity matrix **I** of size $m\times m$ and zero matrix **0** of size $m\times(n-m)$. This can be obtained by introducing linear transformation (49). Note, that this transformation leads to the observable canonical form. Then, state vector $\mathbf{x}(t)$ can be partitioned into the form given by Eq. (66).

The main task of the reduced-order observer is to reconstruct vector $\mathbf{x}_{o2}(t)$. Taking into consideration Eq. (66), system (52) can be presented, as

$$\dot{\mathbf{y}}(t) = \mathbf{A}_{11}\mathbf{y}(t) + \mathbf{A}_{12}\mathbf{x}_{o2}(t) + \mathbf{B}_1\mathbf{u}(t), \quad (73a)$$

$$\dot{\mathbf{x}}_{o2}(t) = \mathbf{A}_{21}\mathbf{y}(t) + \mathbf{A}_{22}\mathbf{x}_{o2}(t) + \mathbf{B}_2\mathbf{u}(t), \quad (73b)$$

where

$$\mathbf{A}_o = \begin{bmatrix} \mathbf{A}_{11} & \mathbf{A}_{12} \\ \mathbf{A}_{21} & \mathbf{A}_{22} \end{bmatrix}, \quad \mathbf{B}_o = \begin{bmatrix} \mathbf{B}_1 \\ \mathbf{B}_2 \end{bmatrix}.$$

To calculate the estimation of vector $\mathbf{x}_{o2}(t)$, Eq. (73a) should be left-side multiplied by matrix **L** of dimensions $(n-m)\times m$ and subtracted from Eq. (73b), yielding

$$\begin{aligned} \dot{\hat{\mathbf{x}}}_{o2}(t) &= (\mathbf{A} - \mathbf{LA})\hat{\mathbf{x}}_{o2}(t) + \mathbf{A}_{21}\mathbf{y}(t) + \\ &+ \mathbf{B}_2\mathbf{u}(t) + \mathbf{L}(\dot{\mathbf{y}}(t) - \mathbf{A}_{11}\mathbf{y}(t)) - \mathbf{LB}_1\mathbf{u}(t) \end{aligned} \quad (74)$$

The block diagram representing the observer given by Eq. (74) is shown in Figure 15.

The first step in designing the observer is to define it in the form given by Eq. (74). Matrix **L** should be chosen in such a way, that matrix $\mathbf{A}_{22} - \mathbf{LA}_{21}$ has the expected real or complex conjugated eigenvalues. In practice the eigenvalues should have negative real parts of the significant magnitude providing that the observer quickly estimates the corresponding state space variables of the system.

Modifying the block diagram from Figure 15 into the form presented in Figure 16, the differentiation of signal $\mathbf{y}(t)$ can be avoided. The modification involves moving the summation block from the input to the output of the integrating element, resulting in the cancelation of the differentiation. Figure 16 presents also the transformation of the state space vector to the form suitable for the recollocation of sensors and actuators.

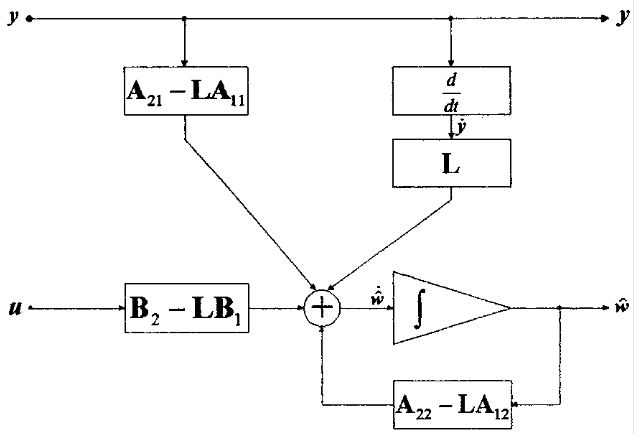

Fig. 15. Reduced-order observer

Finally the observer can be presented in the following form

$$\begin{aligned} \hat{\mathbf{w}}(t) &= (\mathbf{A}_{22} - \mathbf{LA}_{12})\mathbf{w}(t) + (\mathbf{A}_{22} - \mathbf{LA}_{12})\mathbf{Ly}(t) + \\ &+ (\mathbf{A}_{21} - \mathbf{LA}_{11})\mathbf{y}(t) + (\mathbf{B}_2 - \mathbf{LB}_1)\mathbf{u}(t) \end{aligned} \quad (75)$$

where

$$\hat{\mathbf{w}}(t) = \hat{\mathbf{x}}_{o2}(t) - \mathbf{Ly}(t) \quad (76)$$

The approach presented above is not the only way for designing the explicit form of the reduced-order observer. Other methods, such as transformation into the canonical form or hypothesizing about the general structure and solution for unknown parameters can be applied. Algebraically they can be even simpler but the most effective for the recollocation problem is the method presented above.

The theoretical part can be summed up with the following **algorithm** recollocating the axes or planes of measurement to the axes or planes of actuation:

1. Design the state-space model of the examined system using the real locations of sensors, Eqs. (46), (48).
2. Design the state-space model of the same system using the required locations of sensors (collocated with the locations of actuators, Eqs. (60, 61)).
3. Transform the two systems into their canonical observable forms, Eqs. (52), (53) and (63), (64). Partition the state vector into two parts: the real measurement vector, and the required measurement vector, Eq. (66).
4. Design the reduced-order observer for the estimation of this part of the state vector that is not measured directly, Eqs. (75), (76).
5. Calculate transformation matrix **P** and transform the real measurement vector into the required measurement vector, Eqs. (66), (72).

5. ROTOR SUPPORTED BY ACTIVE MAGNETIC BEARINGS

5.1. Model of considered system

Consider again a rigid rotor shown in Figure 1. To simplify the calculations the rotor is assumed to be in its standstill ($\Omega = 0$) and the vibrations in xz and yz planes are supposed to be independent on each other. In this case motion

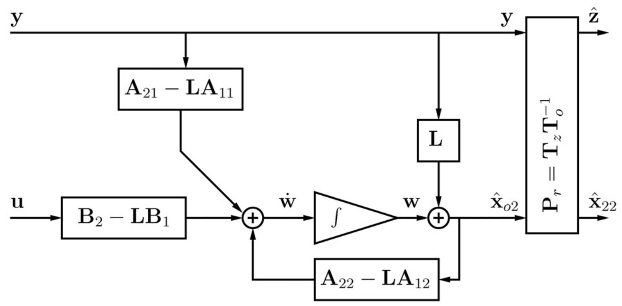

Fig. 16. Improved reduced-order observer and signal transformation

equations (9) for xz plane can be written in the following matrix form

$$\mathbf{M}\ddot{\mathbf{p}}_x(t) = \mathbf{T}_b^T \mathbf{F}_x(t) \tag{77}$$

where: $\mathbf{M} = \begin{bmatrix} m & 0 \\ 0 & I_x \end{bmatrix}$, $\mathbf{F}_x = \begin{bmatrix} F_{ax} \\ F_{bx} \end{bmatrix}$, and $\mathbf{p}_x(t) = \begin{bmatrix} x(t) \\ \beta(t) \end{bmatrix}$.

Forces generated by electromagnets are nonlinear functions of coils current $i(t)$ and shaft displacement $x(t)$. After linearization they can be presented in the following form (for respective coil pairs):

$$\begin{aligned} F_{ax}(t) &= k_{iax} i_{ax}(t) + k_{sax} x_a(t), \\ F_{bx}(t) &= k_{ibx} i_{bx}(t) + k_{sbx} x_b(t). \end{aligned} \tag{78}$$

Usually both radial magnetic bearings are identical and symmetric. In this case we have: $k_i = k_{iax} = k_{ibx}$, $k_x = k_{ax} = k_{bx}$. Then Eqs. (78) can be presented in the following matrix form

$$\mathbf{F}_x(t) = k_i \mathbf{i}_x(t) + k_x \mathbf{p}_{xb}(t) = k_i \mathbf{i}_x(t) + k_x \mathbf{T}_b \mathbf{p}_x(t), \tag{79}$$

where: $\mathbf{i}_x(t) = \begin{bmatrix} i_{ax}(t) \\ i_{bx}(t) \end{bmatrix}$, $\mathbf{p}_{bx}(t) = \begin{bmatrix} x_a(t) \\ x_b(t) \end{bmatrix}$. Then Eq. (77) can be transformed to

$$\mathbf{M}\ddot{\mathbf{p}}_x(t) - k_x \mathbf{T}_b^T \mathbf{T}_b \mathbf{p}_x(t) = k_i \mathbf{T}_b^T \mathbf{i}_x(t) \tag{80}$$

which can be presented as the following state-space equation

$$\begin{bmatrix} \dot{x}_1(t) \\ \dot{x}_2(t) \\ \dot{x}_3(t) \\ \dot{x}_4(t) \end{bmatrix} = \begin{bmatrix} \dot{x}(t) \\ \dot{\beta}(t) \\ \ddot{x}(t) \\ \ddot{\beta}(t) \end{bmatrix} =$$

$$= \begin{bmatrix} 0 & 0 & 1 & 0 \\ 0 & 0 & 0 & 1 \\ \frac{2k_x}{m} & \frac{k_x(b-a)}{m} & 0 & 0 \\ \frac{k_x(b-a)}{I_x} & \frac{k_x(a^2+b^2)}{I_x} & 0 & 0 \end{bmatrix} \begin{bmatrix} x(t) \\ \beta(t) \\ \dot{x}(t) \\ \dot{\beta}(t) \end{bmatrix} + \tag{81}$$

$$+ \begin{bmatrix} 0 & 0 \\ 0 & 0 \\ \frac{k_i}{m} & \frac{k_i}{m} \\ \frac{-k_i a}{I_x} & \frac{k_i b}{I_x} \end{bmatrix} \begin{bmatrix} i_{ax}(t) \\ i_{bx}(t) \end{bmatrix}.$$

The second of (10) is the measurement equation of shaft displacements in Cartesian coordinates. The displacements are measured at real sensor locations. In state-space notation at xz plane Eq. (10) takes the following form

$$\begin{bmatrix} y_1(t) \\ y_2(t) \end{bmatrix} = \begin{bmatrix} 1 & -c & 0 & 0 \\ 1 & d & 0 & 0 \end{bmatrix} \begin{bmatrix} x_1(t) \\ x_2(t) \\ x_3(t) \\ x_4(t) \end{bmatrix}. \tag{82}$$

The first of (10) is also the measurement equation but the displacements are measured at the locations of active magnetic bearings. This is the required equation, as it collocates the planes of sensors into the planes of actuators. In state-space notation at xz plane the required measurement equation takes the following form

$$\begin{bmatrix} z_1(t) \\ z_2(t) \end{bmatrix} = \begin{bmatrix} 1 & -a & 0 & 0 \\ 1 & b & 0 & 0 \end{bmatrix} \begin{bmatrix} x_1(t) \\ x_2(t) \\ x_3(t) \\ x_4(t) \end{bmatrix}. \tag{83}$$

Thus system matrices are as follows

$$\mathbf{A} = \begin{bmatrix} 0 & 0 & 1 & 0 \\ 0 & 0 & 0 & 1 \\ \frac{2k_x}{m} & \frac{k_x(b-a)}{m} & 0 & 0 \\ \frac{k_x(b-a)}{I_x} & \frac{k_x(a^2+b^2)}{I_x} & 0 & 0 \end{bmatrix},$$

$$\mathbf{B} = \begin{bmatrix} \mathbf{B}_1 & \mathbf{B}_2 \end{bmatrix} = \begin{bmatrix} 0 & 0 \\ 0 & 0 \\ \frac{k_i}{m} & \frac{k_i}{m} \\ \frac{-k_i a}{I_x} & \frac{k_i b}{I_x} \end{bmatrix} \tag{84}$$

$$\mathbf{C} = \begin{bmatrix} \mathbf{C}_1 \\ \mathbf{C}_2 \end{bmatrix} = \begin{bmatrix} 1 & -c & 0 & 0 \\ 1 & d & 0 & 0 \end{bmatrix},$$

$$\mathbf{B}_C^T = \begin{bmatrix} \mathbf{B}_{C1} \\ \mathbf{B}_{C2} \end{bmatrix} = \begin{bmatrix} 1 & -a & 0 & 0 \\ 1 & b & 0 & 0 \end{bmatrix}$$

5.2. Analitical calculations

Observability matrices of the system (52), (63) are as follows

$$\mathbf{S}_o = \left[\mathbf{C}_1, \mathbf{C}_2, \mathbf{C}_1\mathbf{A}, \mathbf{C}_2\mathbf{A}, \mathbf{C}_1\mathbf{A}^2, \mathbf{C}_2\mathbf{A}^2, \mathbf{C}_1\mathbf{A}^3, \mathbf{C}_2\mathbf{A}^3\right]^T$$

$$\mathbf{S}_z = \left[\mathbf{B}_{\mathbf{C}1}, \mathbf{B}_{\mathbf{C}2}, \mathbf{B}_{\mathbf{C}1}\mathbf{A}, \mathbf{B}_{\mathbf{C}2}\mathbf{A}, \mathbf{B}_{\mathbf{C}1}\mathbf{A}^2, \mathbf{B}_{\mathbf{C}2}\mathbf{A}^2, \mathbf{B}_{\mathbf{C}1}\mathbf{A}^3, \mathbf{B}_{\mathbf{C}2}\mathbf{A}^3\right]^T.$$

After several calculations required observability matrix $\mathbf{S}_z$ can be presented as

$$\mathbf{S}_z = \begin{bmatrix} 1 & -c & 0 & 0 \\ 1 & d & 0 & 0 \\ 0 & 0 & 1 & -c \\ 0 & 0 & 1 & d \\ \frac{2k_x}{m} - \frac{ck_x(b-a)}{I_x} & \frac{k_x(b-a)}{m} - \frac{ck_x(a^2+b^2)}{I_x} & 0 & 0 \\ \frac{2k_x}{m} + \frac{dk_x(b-a)}{I_x} & \frac{k_x(b-a)}{m} + \frac{dk_x(a^2+b^2)}{I_x} & 0 & 0 \\ 0 & 0 & \frac{2k_x}{m} - \frac{ck_x(b-a)}{I_x} & \frac{k_x(b-a)}{m} - \frac{ck_x(a^2+b^2)}{I_x} \\ 0 & 0 & \frac{2k_x}{m} + \frac{dk_x(b-a)}{I_x} & \frac{k_x(b-a)}{m} + \frac{dk_x(a^2+b^2)}{I_x} \end{bmatrix}$$

It can be shown that observability matrices $\mathbf{S}_z$ and $\mathbf{S}_o$ are almost the same, except constants a, b that are replaced by c, d. Furthermore, it can be shown that the first four rows of observability matrices $\mathbf{S}_o$ and $\mathbf{S}_z$ form the following transformation matrices

$$\mathbf{T}_o = \begin{bmatrix} 1 & -c & 0 & 0 \\ 1 & d & 0 & 0 \\ 0 & 0 & 1 & -c \\ 0 & 0 & 1 & d \end{bmatrix}, \quad \mathbf{T}_z = \begin{bmatrix} 1 & -a & 0 & 0 \\ 1 & b & 0 & 0 \\ 0 & 0 & 1 & -a \\ 0 & 0 & 1 & b \end{bmatrix}.$$

Thus, transformation matrix $\mathbf{P}_r$ given by Eq. (67) takes the following form

$$\mathbf{P}_r = \mathbf{T}_z\mathbf{T}_o^{-1} = \begin{bmatrix} \frac{d+a}{c+d} & \frac{c-a}{c+d} & 0 & 0 \\ \frac{d-b}{c+d} & \frac{c+b}{c+d} & 0 & 0 \\ 0 & 0 & \frac{d+a}{c+d} & \frac{c-a}{c+d} \\ 0 & 0 & \frac{d-b}{c+d} & \frac{c+b}{c+d} \end{bmatrix}.$$

We can see that unknown transformation matrix $\mathbf{P}_r$ is a combination of two zero matrices and two matrices $\mathbf{P}$ introduced in (Gosiewski *et al.* 2010) and repeated in Eq. (14). This combination has the following form

$$\mathbf{P}_r = \begin{bmatrix} \mathbf{P} & \mathbf{0} \\ \mathbf{0} & \mathbf{P} \end{bmatrix} \tag{85}$$

Upper non-zero submatrix $\mathbf{P}$ transforms displacements while lower non-zero submatrix $\mathbf{P}$ transforms velocities of the shaft. Both submatrices are the same, as are the displacement and velocity modeshapes of the rigid rotor. Because of zero submatrices in Eq. (85) the transformation of displacements does not require estimated velocities and vice versa. If all displacements are measured, as it is in the example above, the state observer can be omitted.

5.3. Numerical calculations

Computer simulations were carried out for the following rotor and bearing parameters: m = 18.5 kg, I_z = 0.0115 kgm^2, I_x = 0.6525 kgm^2, $k_s = 1.6024\times10^6$ N/m, k_i = 100.1483 A/m, l = 0.902 m, $a = 0.6l$, $b = l - a$, $c = 0.7l$, $d = 0.3l$. System matrices are as follows

$$\mathbf{A} = \begin{bmatrix} 0 & 0 & 1 & 0 \\ 0 & 0 & 0 & 1 \\ 0 & -15600 & 0 & 0 \\ -443000 & 1039000 & 0 & 0 \end{bmatrix},$$

$$\mathbf{B} = \begin{bmatrix} 0 & 0 \\ 0 & 0 \\ 5.4134 & 5.4134 \\ -83.0655 & 55.3770 \end{bmatrix},$$

$$\mathbf{C} = \begin{bmatrix} 1.0000 & -0.6314 & 0 & 0 \\ 1.0000 & 0.2706 & 0 & 0 \end{bmatrix},$$

$$\mathbf{B}_{\mathbf{C}}^{T} = \begin{bmatrix} 1.0000 & -0.5412 & 0 & 0 \\ 1.0000 & 0.3608 & 0 & 0 \end{bmatrix}.$$

Transformation matrices

$$\mathbf{T}_o = \begin{bmatrix} 1.0000 & -0.6314 & 0 & 0 \\ 1.0000 & 0.2706 & 0 & 0 \\ 0 & 0 & 1.0000 & -0.6314 \\ 0 & 0 & 1.0000 & 0.2706 \end{bmatrix},$$

$$\mathbf{T}_z = \begin{bmatrix} 1.0000 & -0.5412 & 0 & 0 \\ 1.0000 & 0.3608 & 0 & 0 \\ 0 & 0 & 1.0000 & -0.5412 \\ 0 & 0 & 1.0000 & 0.3608 \end{bmatrix},$$

yield the following canonical form

$$\mathbf{C}_o = \begin{bmatrix} 1 & 0 & 0 & 0 \\ 0 & 1 & 0 & 0 \end{bmatrix}, \quad \mathbf{C}_z = \begin{bmatrix} 1 & 0 & 0 & 0 \\ 0 & 1 & 0 & 0 \end{bmatrix}.$$

Transformation matrix from the non-collocated to the collocated system can be presented as

$$\mathbf{P}_r = \mathbf{T}_z \mathbf{T}_o^{-1} = \begin{bmatrix} 0.9000 & 0.1000 & 0 & 0 \\ -0.1000 & 1.1000 & 0 & 0 \\ 0 & 0 & 0.9000 & 0.1000 \\ 0 & 0 & -0.1000 & 1.1000 \end{bmatrix}.$$

while matrix **P** calculated from Eq. (3.6) is as follows

$$\mathbf{P} = \mathbf{T}_b \mathbf{T}_m^{-1} = \begin{bmatrix} 0.9000 & 0.1000 \\ -0.1000 & 1.1000 \end{bmatrix}.$$

As we can see transformation matrix $\mathbf{P}_r$ is a combination of zeros and matrices **P** introduced in (Gosiewski *et al.* 2010). This confirms analytical results obtained in previous section.

6. CONCLUSIONS

The paper presents a new method for calculating measurement signals at axes or planes of actuation given real signals taken at the axes or planes of measurement. The method was called *recollocation method*. The algorithm recollocating the axes or planes of measurement to the axes or planes of actuation was developed. The proposed approach is based on some techniques known from the control systems theory:

- transformations to canonical forms,
- state observers.

As an example of the non-collocated system, a rigid rotor with sensors located at some distance from magnetic bearings was considered. Transformation matrices recollocating measurement signals from sensors to bearings locations were calculated analytically and numerically. The results were compared with the results obtained in (Gosiewski 2010) for the different method. This comparison confirmed the correctness of the new method.

The state observer was not required for the rotor as the transformations result rather from the geometry of the structure (its modeshapes (Gosiewski *et al.* 2010)) but not from its dynamics (time characteristics). Consequently the transformations for displacements and for velocities are the same. The observer should be used only when the number of measurement signals is lower than the number of displacements, what was established in (Gosiewski *et al.* 2010).

Future research should focus on the verification of the proposed method. The method should be tested with the vibration control system of the flexible structure with many degrees of freedom using the following techniques:

- finite element analysis,
- model order reduction (e.g. modal order reduction),
- state observers,
- various control techniques.

The verification should be performed by computer simulations as well as by experimental investigations. Especially the comparison of the quality and stability of the non-collocated and recollocated system would be very interesting.

References

Buhr C., Franchek A., Bernhard R.J. 1997, *Non-collocated adaptive-passive vibration control*. Journal of Sound and Vibration, 206 (3), pp. 371–398.

Gosiewski Z. 2004, *Diagnostic of Rotating Machinery with Magnetic Bearings & Rigid Rotor*. 9th Int. Symp. Magnetic Bearings, Lexington, Kentucky, USA, August.

Gosiewski Z. 2008, *Control-oriented modelling and control of rotor vibration*. Acta Mechanica & Automatica, vol. 2, No. 2, Białystok.

Gosiewski Z. 2010, *Analytical analysis of MIMO magnetic bearing-rotor system*. Proc. of the 8th IFToMM International Conference on Rotordynamics, September 12–15, KIST, Seoul, Korea.

Gosiewski Z., Falkowski K. 2003, *Wielofunkcyjne łożyska magnetyczne Multifunction magnetic bearings*. Monografia nr 19, Biblioteka Naukowa Instytutu Lotnictwa (in Polish).

Gosiewski Z., Kulesza Z., Siemieniako F. 2010, *Analytical methods for sensors and actuators recollocation in vibration control systems*. Proc. of the 8th IFToMM International Conference on Rotordynamics, September 12–15, KIST, Seoul, Korea.

Kaczorek T. 1983, *Teoria wielowymiarowych układów dynamicznych liniowych*. WNT, Warszawa.

Meirovitch L., Baruh H. 1983, *On the problem of observation spillover in self-adjoint distributed-parameters systems*. Journal of Optimization Theory and Applications, 39 (2).

Nordstrom L.J.L., Nordberg T.P. 2004, *A time delay method to solve non-collocated input estimation problems*. Mechanical Systems and Signal Processing, 18, pp. 1469–1483.

Preumont A. 2002, *Vibration control of active structures: an introduction*. Kluwer Academic Publishers, Dordrecht.

Qiu Z-C., Han J-D., Zhang X-M., Wang Y-C., Wu Z-W. 2009, *Active vibration control of a flexible beam using a non-collocated acceleration sensor and piezoelectric patch actuator*. Journal of Sound and Vibration, 326, pp. 438–355.

Schweitzer G. 2002, *Active magnetic bearings – chances and limitations*. 8th Int. Symp. Magnetic Bearings, Mito, Japan.

Weng M.-C., Lu X., Trumper D.L. 2002, *Vibration control of flexible beams using sensor averaging and actuator averaging methods.* IEEE Transactions on Control Systems Technology, 10 (4), pp. 568–577.